
Cross-Tokenizer Distillation via Approximate Likelihood Matching

Benjamin Minixhofer^{0x43} Ivan Vulić^{0x43} Edoardo M. Ponti^{0x45,0x43}
^{0x43}University of Cambridge ^{0x45}University of Edinburgh

Abstract

Distillation has shown remarkable success in transferring knowledge from a Large Language Model (LLM) teacher to a student LLM. However, current distillation methods predominantly require the same tokenizer between the teacher and the student, restricting their applicability to only a small subset of teacher–student pairs. In this work, we develop a cross-tokenizer distillation method to solve this crucial deficiency. Our method is the first to enable cross-tokenizer distillation without a next-token prediction loss as the main objective, instead purely maximizing the student predictions’ similarity to the teacher’s predictions (known as *pure* distillation), while also being robust to large mismatches between the teacher and the student tokenizer function and vocabulary. Empirically, our method enables substantially improved performance as tested on two use cases. First, we show that viewing tokenizer transfer as self-distillation enables unprecedentedly effective transfer across tokenizers. We transfer (subword-level) Llama and Gemma models to byte-level tokenization more effectively than prior methods transfer to a similar subword tokenizer under a comparable training budget. Transferring different base models to the same tokenizer also enables ensembling them (e.g., via averaging their predicted probabilities) which boosts performance. Second, we use our cross-tokenizer distillation method to distil a large maths-specialized LLM into a smaller model, achieving competitive maths problem-solving performance. Overall, our results make substantial strides toward better adaptability and enhanced interaction between different LLMs.

1 Introduction

Even the latest, most powerful Large Language Models (LLMs) still operate on *tokens*, and therefore require a *tokenizer* — a manually designed component which turns text into a sequence of tokens. Most currently available language models use subword tokenization (Sennrich et al., 2016; Kudo & Richardson, 2018), where each token is a word, or part of a word. Even though subword tokenizers are currently dominant, they are heterogeneously implemented: when a model is released, it often comes with its own tokenizer which has distinct properties such as which tokens it comprises (its *vocabulary*) and which method is used to segment text into these tokens (its *tokenization function*). Furthermore, there has been a recent trend away from subwords toward models using vocabularies consisting of characters (Tay et al., 2022; Nawrot et al., 2023) or bytes (e.g. Xue et al., 2022; Yu et al., 2023; Pagnoni et al., 2024). This exemplifies the wildly diverse landscape of tokenization.

On the other hand, distillation (Buciluă et al., 2006; Hinton et al., 2015) has emerged as a powerful paradigm for creating effective language models by training them based on the signal from another model. Distillation allows, for example, compressing a large language model (the *teacher*) into a smaller model (the *student*) while retaining the teachers’ abilities to a large extent (Gu et al., 2024). However, existing distillation methods predominantly assume that both teacher and student represent their input in the same way, i.e., that their tokenizer is the same. This strongly limits their applicability

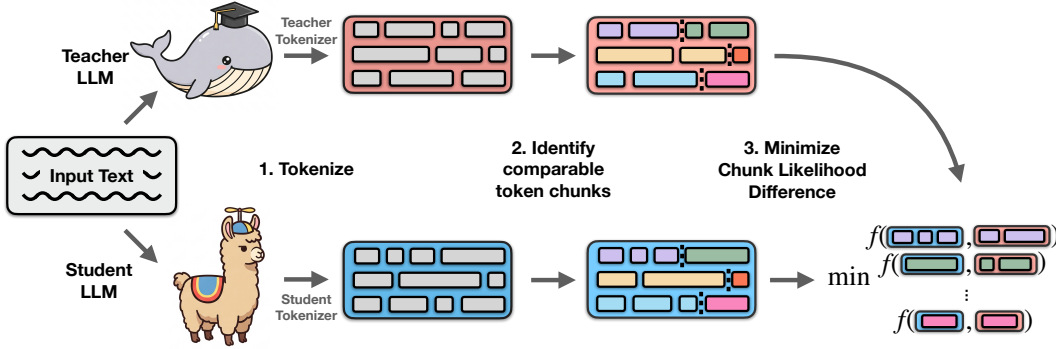


Figure 1: We propose a cross-tokenizer distillation method which identifies chunks of tokens which are *approximately comparable* (c.f. Section 3), then minimizes the differences between their likelihoods.

to only a small subset of all the possible teacher–student pairs of existing models. In this work, we develop a *cross-tokenizer distillation* method to solve this problem. Prior cross-tokenizer distillation methods heuristically incorporate information from the teacher alongside a main objective (e.g., next-token prediction; Zhang et al., 2024; Wan et al., 2024; Boizard et al., 2025). In contrast, our objective enables *pure* distillation — training to purely match the teachers’ behaviour, instead of matching the teachers’ behaviour as an auxiliary objective. This leads to attractive theoretical properties (Section 3) as well as empirical improvements (Section 4), while also being robust to highly dissimilar teacher and student tokenizers (e.g., distilling from a subword tokenizer to a byte-level tokenizer).

In a nutshell, given some text, we first tokenize it with the teacher and the student tokenizers and compute the next-token likelihoods of all tokens under the teacher and the student models. We then find aligned chunks of tokens (i.e., the chunks encoding the same portions of text) between the two sequences. Now, to compare the chunk likelihoods of the aligned chunks (e.g., via their KL-divergence), we would need to know the likelihoods of all possible outcomes. This is not an issue in the typical (same-tokenizer) distillation case since we can compute the likelihoods of all tokens in the vocabulary in a single forward pass. However, in our case, we would have to compute the likelihoods of all multi-token chunks, which is impossible since their number is infinite. Thus, we approximate the chunk likelihood difference via a binarised f -divergence (c.f. Section 3). Unfortunately, a problem remains: even if two chunks of tokens encode the same text, their likelihoods may not be comparable since the two token sequences can leak different information about the future contents of the text (this has been termed *tokenization bias*, see Section 2.1).¹ Thus, we introduce a method to approximate the tokenization bias difference between chunks of tokens to identify *approximately comparable* chunks (Section 3.1). Together, these steps lead to an effective cross-tokenizer distillation method, which we refer to as Approximate Likelihood Matching (ALM), sketched in Figure 1.

We empirically test ALM on two main use cases. First, we propose a novel viewpoint of tokenizer transfer as cross-tokenizer self-distillation, which ALM excels at (Use Case 1). This enables transferring subword-based LLMs to a different subword tokenizer while largely retaining performance. We further show that transferring different models to the same subword tokenizer enables ensembling their predictions (e.g., via averaging their logits) which substantially boosts performance over the individual parts. Moreover, we demonstrate that tokenizer transfer self-distillation via ALM enables a first instance of subword-to-byte distillation, where we retrofit an existing (subword-based) LLM to operate at the byte-level instead, creating a competitive byte-level model at a fraction of the cost of training from scratch. Secondly, we show that ALM outperforms prior methods at cross-tokenizer distillation of a large math-specialized model into a much smaller model (Use Case 2). This paves the way toward greatly expanding the number of possible teacher–student pairs for distillation, improving reusability, composability and transferability of language models (c.f. Pfeiffer et al., 2023; Raffel, 2023). Our code and models are publicly available at github.com/bminixhofer/aln.

¹For example, assuming a vocabulary of English words, the token sequence $\{_Hello, _World\}$ leaks that there is no ‘d’ after ‘_World’, otherwise the text would have been tokenized as $\{_Hello, _World\}$ instead.

2 Preliminaries and Background

2.1 Tokenizers

Definition. Tokenizers map the input text to a sequence of tokens. Formally, they operate on finite sequences Σ^* over the alphabet Σ . For simplicity and since it is not vital to our method, we presume Σ to be the set of bytes $\{0, \dots, 255\}$ and Σ^* a string represented as bytes via the UTF-8 standard (Yergeau, 2003). This does not lose generality, since although some tokenizers operate on units built on top of UTF-8 bytes (e.g., Unicode characters; Kudo & Richardson, 2018), they can be transformed to operate on bytes instead (Minixhofer et al., 2024). Following prior work (Uzan et al., 2024; Feher et al., 2024), we denote the tokenizer as the tuple (\mathcal{V}, T) comprising (i) the vocabulary \mathcal{V} which determines the set of all possible tokens and (ii) the tokenization function $T : \Sigma^* \rightarrow \mathcal{V}^*$ which determines the sequence of tokens any given text is mapped to.

Tokenization functions fuse bytes into larger (e.g., subword) tokens without loss of information.² Consider the tokens $\{t_1, t_2, \dots, t_n\} = T(\mathbf{x})$. Then $t_1 \odot t_2 \odot \dots \odot t_n = \mathbf{x}$ (where \odot is the concatenation operator). This has multiple useful implications. All elements in the vocabulary \mathcal{V} are sequences of bytes Σ^* .³ Furthermore, T is injective so there exists a left inverse D such that $\mathbf{x} = D(T(\mathbf{x})) \forall \mathbf{x}$. We call D the *detokenization function*. Importantly, D is only a *left* inverse, i.e., there may exist a token sequence \mathbf{t} such that $\mathbf{t} \neq T(D(\mathbf{t}))$ since T is not necessarily bijective.

Tokenization Bias. Subword tokenizers suffer from what has been termed *tokenization bias* (Phan et al., 2024): sequences of tokens can implicitly leak information about the future content of the text they tokenize. For example, assuming a vocabulary of English words, the token sequence $\{_Hello, _World\}$ leaks that there is no ‘d’ after ‘_World’, otherwise the text would have been tokenized as $\{_Hello, _World\}$ instead (see also Vieira et al., 2024). We can measure tokenization bias via the notion of cover encodings (Phan et al., 2024). The cover encodings of a sequence of tokens $\mathbf{t} = T(\mathbf{x})$ are all sequences of tokens \mathbf{u} such that (i) decoding and re-encoding the sequence leads to the same token sequence $T(D(\mathbf{u})) = \mathbf{u}$ (this has been referred to as *validity*), (ii) \mathbf{x} is a prefix of $D(\mathbf{u})$ and (iii) \mathbf{x} is not a prefix of $D(\mathbf{u}_{0:|\mathbf{u}|-1})$ (i.e., the last token in \mathbf{u} covers a part of \mathbf{x}).⁴ We denote the set of all cover encodings as $\text{cover}(\mathbf{t})$. Note that $\mathbf{t} \in \text{cover}(\mathbf{t})$. We further define the set of *implied exclusions* $\mathcal{X}(\mathbf{t}) = \{D(\mathbf{u}) \mid \mathbf{u} \in \text{cover}(\mathbf{t}), \mathbf{u} \neq \mathbf{t}\}$. $|\mathcal{X}(\mathbf{t})|$ is a concrete measure of the tokenization bias of any particular token sequence \mathbf{t} . If we observe the token sequence $\mathbf{t} = T(\mathbf{x})_{:i}$, we know that $\mathbf{x} \notin \mathcal{X}(\mathbf{t})$. Otherwise, \mathbf{x} would have been tokenized differently. In our previous example, $_Hello_World \in \mathcal{X}(\{_Hello, _World\})$. Not all tokenizers exhibit tokenization bias, e.g., the byte-level tokenization $T(\mathbf{x}) = \mathbf{x}$ is unbiased.⁵ However, the predominantly used subword tokenization methods BPE (Sennrich et al., 2016) and UnigramLM (Kudo & Richardson, 2018), among others, do suffer from tokenization bias.

2.2 Generative Language Models

Generative language models are auto-regressive next-token predictors. Given a sequence of tokens, a generative language model θ defines a probability distribution $p_\theta(t_i | \mathbf{t}_{:i})$ ⁶ over the next token. To compute the probability of a multi-token sequence conditioned on \mathbf{t}_i , we can compute $p_\theta(\mathbf{t}_{i:j} | \mathbf{t}_{:i}) = p_\theta(t_i | \mathbf{t}_{:i}) \cdot \dots \cdot p_\theta(t_{j-1} | \mathbf{t}_{:j-1})$. To auto-regressively sample from the model, we continuously sample $u \sim p_\theta(u | \mathbf{t}_{:i})$ and append the sampled u to the sequence. However, the token level is not an intuitive interface to language models. To interface with language models at the *text* level, we need to wrap the language model with tokenization and detokenization. We can compute the probability of a text \mathbf{y} conditioned on the text \mathbf{x} via $p_\theta(T(\mathbf{y}) | T(\mathbf{x}))$. We can auto-regressively generate a text \mathbf{y} conditioned on \mathbf{x} by sampling $u_i \sim p_\theta(u_i | T(\mathbf{x}) \odot \mathbf{u}_{:i})$ for $i \in \{0, \dots, n\}$, then detokenizing to obtain

²This is not the case for tokenizers which can emit `<unk>` due to out-of-vocabulary characters (such as the original BERT tokenizer; Devlin et al., 2019). However, a tokenizer with this property can again be converted to byte-level and the vocabulary minimally extended to cover all bytes to restore the byte fusion property.

³For ease of notation, we do not treat special tokens (such as an `<eos>` token marking the end of the text) separately. Special tokens can be considered a part of the encoding Σ , e.g., a range from $\{256, \dots, 256 + k\}$.

⁴See Phan et al. (2024) for a more detailed exposition of cover encodings.

⁵Unbiasedness is connected to the notion of *incrementality* introduced in BLT (Pagnoni et al., 2024). We prove in Appendix A.1 that incrementality implies unbiasedness, but do not further use incrementality.

⁶We use Python-style indexing where $\mathbf{t}_{i:j}$ indicates the elements in \mathbf{t} starting from i up to but excluding j , and $\mathbf{t}_{:j}$ indicates the elements from the beginning (index 0) up to but excluding j .

$\mathbf{y} = D(u_0, \dots, u_n)$. However, crucially, for the tokenization and detokenization transformations to be valid (i.e., not to introduce any bias), $T(\mathbf{x}) \odot T(\mathbf{y}) = T(\mathbf{x} \odot \mathbf{y})$ must hold. This is not always the case due to tokenization bias (see above).

2.3 Distillation

Pure Distillation vs. Hybrid Distillation. The general idea behind distillation is to transfer knowledge from a teacher model ϕ to a student model θ , where the student model has some desirable properties (e.g., being more efficient; Buciluă et al., 2006; Hinton et al., 2015). We denote the teacher likelihoods $p_T := p_\phi$ and the student likelihoods $p_S := p_\theta$. A key distinction can be drawn between *pure* distillation, where the primary objective is for the student predictions $p_S(\mathbf{y}|\mathbf{x})$ to match the teachers’ predictions $p_T(\mathbf{y}|\mathbf{x})$ and *hybrid* distillation, where the main task is to model some ground-truth $p(\mathbf{y}|\mathbf{x})$, and a distillation objective is used in addition to the main objective (e.g., next-token prediction) to increase performance on the main task. Hybrid distillation can be useful to avoid potential issues arising from the pure setup, e.g. teacher hacking (Tiapkin et al., 2025) and a detrimental student–teacher capacity gap (Busbridge et al., 2025). On the other hand, pure distillation can be highly effective at preserving the student’s knowledge when the teacher and the student have the same underlying backbone (in case of *self-distillation*); a setting where hybrid distillation can be highly destructive, as we find later in Section 4.

Distillation Objectives. To encourage the student predictions to match the teachers’, we need some measure of distance between $p_S(\mathbf{y}|\mathbf{x})$ and $p_T(\mathbf{y}|\mathbf{x})$. The typical choice is the Kullback-Leibler divergence $D_{\text{KL}}(p_T \parallel p_S) = \sum_{t_i \in \mathcal{V}} p_T(t_i|\mathbf{t}_{:i}) \log \frac{p_T(t_i|\mathbf{t}_{:i})}{p_S(t_i|\mathbf{t}_{:i})}$ (Kullback & Leibler, 1951). However, other objectives have been argued to be more suitable for distillation (Gu et al., 2024; Ko et al., 2024); many of them are instances of f -divergences of the form $D_f(p_T \parallel p_S) = \sum_{t_i \in \mathcal{V}} f(p_T(t_i|\mathbf{t}_{:i}) \| p_S(t_i|\mathbf{t}_{:i}))$ where $f(p_T(x) \| p_S(x)) = p_S(x)g(\frac{p_T(x)}{p_S(x)})$ and g is convex and non-negative (Rényi, 1961).⁷

Cross-Tokenizer Distillation. Recent work has begun investigating ways to distill across different tokenizers. ULD (Boizard et al., 2025) trains the student via next-token prediction plus a Wasserstein distance loss (Kantorovich, 1960) between the teacher logits and the student logits at every step. This ensures that the absolute difference between the sorted teacher logits and sorted student logits at every position is small. MinED (Wan et al., 2024) aligns the student and teacher logits by greedily aligning every token in the students’ vocabulary with the teacher token which has the minimal Levenshtein edit distance (Levenshtein, 1966) to the student token. The main objective is again minimizing cross-entropy of the next-token prediction, but the KL-divergence between the student logits and aligned teacher logits is added at every position where there is a one-to-one alignment between the elements of the student and teacher sequences. DSKD (Zhang et al., 2024) projects the student representations to the teacher sequence and the teacher representations to the student sequence via a cross-attention mechanism, then adds the KL-divergence between the teacher predictions and the student-to-teacher projected predictions (and vice versa) to the next-token prediction loss. All existing cross-tokenizer distillation methods heuristically incorporate some information from the teacher. They thus strictly operate in the hybrid distillation setup; they lack the properties necessary to form a pure distillation objective (e.g., the loss being minimised iff $p_S(\mathbf{y}|\mathbf{x}) = p_T(\mathbf{y}|\mathbf{x}) \forall \mathbf{x}, \mathbf{y}$). Our key contribution is introducing a distillation objective which enables pure cross-tokenizer distillation. As we show later in Section 4, pure cross-tokenizer distillation is effective in cases where hybrid distillation can be highly destructive, and, foreshadowing, performs much better in our experiments.

3 Methodology

Our key goal is for the student likelihood $p_S(T_S(\mathbf{z})|T_S(\mathbf{y}))$ to be equal to the teacher likelihood $p_T(T_T(\mathbf{z})|T_T(\mathbf{y}))$ for every prefix $\mathbf{y} \in \Sigma^*$ and continuation $\mathbf{z} \in \Sigma^*$ if the teacher and student token sequences are biased in the same way, i.e., $\mathcal{X}(T_S(\mathbf{y})) = \mathcal{X}(T_T(\mathbf{y}))$ and $\mathcal{X}(T_S(\mathbf{z})) = \mathcal{X}(T_T(\mathbf{z}))$ (c.f. Section 2.1). To this end, we start by computing the next-token probabilities $p_T(T_T(\mathbf{x})_i | T_T(\mathbf{x})_{:i})$

⁷Note that while the divergence induced by f is typically defined as $D_f(p||q) = \sum_x q(x)f(\frac{p(x)}{q(x)})$ we define it as $D_f(p||q) = \sum_x f(p(x)||q(x))$ to retain clarity in absence of the f -divergence viewpoint.

and $p_S(T_S(\mathbf{x})_i | T_S(\mathbf{x})_{:i})$. This can be done in a single forward pass over both language models. We can now find aligned token chunks between the teacher and the student sequences.⁸

$$A_c(\mathbf{x}) = \left\{ (i, j, k, l) \in \mathbb{Z}^4 \left| \begin{array}{l} D(T_T(\mathbf{x})_{:i}) = D(T_S(\mathbf{x})_{:k}) = \mathbf{y}, \\ D(T_T(\mathbf{x})_{i:j}) = D(T_S(\mathbf{x})_{k:l}) = \mathbf{z}, \\ c(\mathbf{y}, \mathbf{z}) \text{ holds} \end{array} \right. \right\} \quad (\text{Alignment Indices})$$

Here, the constraint $c(\mathbf{y}, \mathbf{z})$ forces the probabilities of aligned chunks of tokens to be comparable. The precise definition of this constraint is discussed later in Section 3.1. For now, we define the chunk-level probabilities $p(\mathbf{x}, i:j)$ as

$$p(\mathbf{x}, i:j) := p(T(\mathbf{x})_{i:j} | T(\mathbf{x})_{:i}). \quad (\text{Chunk-Level Probability})$$

This lets us define our final objective minimising a divergence between the chunk-level probabilities:

$$\mathcal{L}^{\text{ALM}}(\mathbf{x}) = \sum_{i,j,k,l \in A_c(\mathbf{x})} f(p_T(\mathbf{x}, i:j)^{\frac{1}{\tau}} \| p_S(\mathbf{x}, k:l)^{\frac{1}{\tau}}) + f(1 - p_T(\mathbf{x}, i:j)^{\frac{1}{\tau}} \| 1 - p_S(\mathbf{x}, k:l)^{\frac{1}{\tau}}) \quad (\text{ALM Objective})$$

where τ is a temperature scaling hyperparameter and f is a function such that, when summed over all possible outcomes $\mathbf{x} \in \Sigma^*$, it would induce an f -divergence (Rényi, 1961). Typically, with identical tokenizers, the sum of the f -divergence would range over all tokens in the vocabulary; however, when comparing chunk-level probabilities there is an infinite amount of possible outcomes since there is an infinite amount of possible byte sequences, which cannot be enumerated and whose probability cannot be estimated in a finite time. We thus resort to computing the f -divergence over the binarized possibilities $\{p(\mathbf{x}, i:j), 1 - p(\mathbf{x}, i:j)\}$ given a sample $\mathbf{x} \sim \mathcal{D}$. This constitutes an upper bound to the true f -divergence and preserves its crucial properties (e.g., being minimal iff $p_S = p_T$; c.f. Appendix A.2 for further analysis). In practice, we choose f as $f_{\text{KL}}(p_T \| p_S) = p_T \log \frac{p_T}{p_S}$ to recover the KL-divergence and ablate the impact of the choice of f and τ in Appendix B.2.

3.1 A Scalar Quantity Measuring Tokenization Bias

As stated above, we would like to constrain alignment such that the prefix and continuation are biased in the same way, i.e., $\mathcal{X}(T_S(\mathbf{y})) = \mathcal{X}(T_T(\mathbf{y}))$ and $\mathcal{X}(T_S(\mathbf{z})) = \mathcal{X}(T_T(\mathbf{z}))$. Unfortunately, this requirement is prohibitively stringent in practice: for example, if the student tokenizer is unbiased while the teacher tokenizer is not, it might rarely (if ever) be fulfilled. We thus define a relaxation which lets us define the alignment constraint $c(\mathbf{y}, \mathbf{z})$ such that the chunk bias differences are *small enough*, but not necessarily zero. To this end, we introduce a precomputable scalar approximation of the difference in tokenization bias between two sequences. Let us consider arbitrary language models A and B (not necessarily a teacher and a student). We first define $(\mathcal{X}_A \setminus \mathcal{X}_B)(\mathbf{x})$ to be the set difference of implied exclusions \mathcal{X} on some text \mathbf{x} between the token sequences of the two i.e. $(\mathcal{X}_A \setminus \mathcal{X}_B)(\mathbf{x}) = \mathcal{X}(T_A(\mathbf{x})) \setminus \mathcal{X}(T_B(\mathbf{x}))$. We can then quantify a scalar difference $b_{A\|B}(\mathbf{x})$ in tokenization bias between the two sequences.

$$b_{B\|A}(\mathbf{x}) = \sum_{\mathbf{d} \in (\mathcal{X}_A \setminus \mathcal{X}_B)(\mathbf{x})} p_A(T_A(\mathbf{d}))$$

⁸We compute *greedy* alignments, i.e., we do not consider partially overlapping alignments, and we make sure the chunks always span the entire text (i.e., if $c(\mathbf{y}, \mathbf{z})$ is never satisfied, there is one chunk spanning from the first to the last token). To implement the alignment algorithm, we take advantage of the fact that both token sequences encode the same bytes. It is thus possible to compute alignments in a single pass via indices (i, k) , where i is increased as long as the token at position i in one sequence ends earlier than the token at position j in the other sequence, and vice versa, and indices are stored if both tokens end at the same byte position. This is in contrast to more complex approaches used in prior work (Fu et al., 2023; Wan et al., 2024): they minimize edit distance between alignments via variants of the Needleman-Wunsch algorithm (Needleman & Wunsch, 1970). This is not necessary if the tokenizers have first been converted to the byte level.

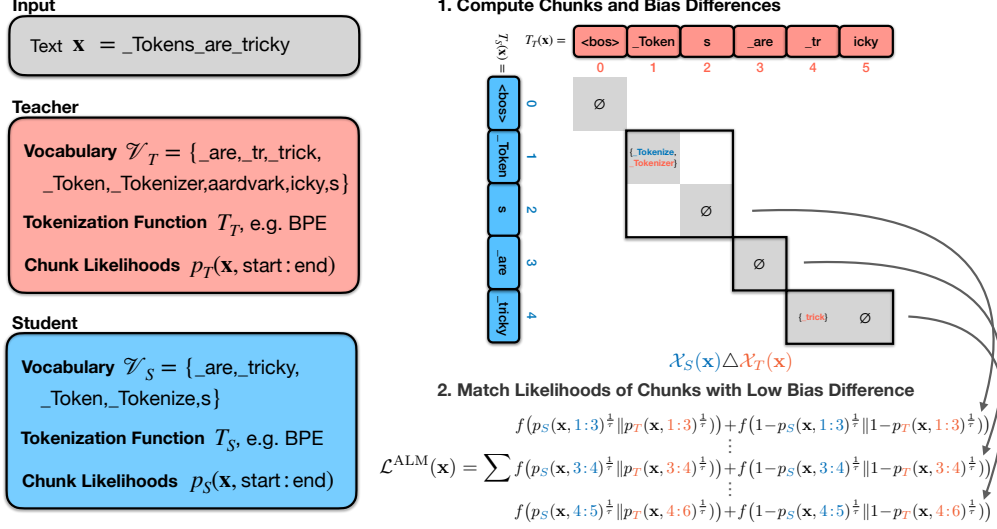


Figure 2: Our method enables effective cross-tokenizer distillation by (1) computing aligned chunks of tokens and their bias differences (2) learning to match the likelihoods of approximately comparable chunks with low bias differences. $\mathcal{X}_S \Delta \mathcal{X}_T$ denotes the symmetric difference between the implied exclusions of the teacher and the student.

If $(\mathcal{X}_A \setminus \mathcal{X}_B)(\mathbf{x}) = \emptyset$, $T_A(\mathbf{x})$ is biased to a lesser or equal extent as $T_B(\mathbf{x})$ and $b_{B\|A}(\mathbf{x}) = 0$. If not, $b_{B\|A}(\mathbf{x})$ will be high if any text \mathbf{d} which T_A is biased against but T_B is not is assigned a high probability by the language model A . Instead, if a text $\mathbf{d} \in (\mathcal{X}_A \setminus \mathcal{X}_B)(\mathbf{x})$ is assigned a low likelihood, it affects the bias difference to a lesser extent. We can use the symmetrized bias $b_{A,B}(\mathbf{x}) = \max(b_{B\|A}(\mathbf{x}), b_{A\|B}(\mathbf{x}))$ as a measure of the ‘biasedness’ of any text. However, computing $b_{B\|A}(\mathbf{x})$ is prohibitively expensive since we need to compute the cover encodings of every text \mathbf{x} under both tokenization functions, as well as the likelihood assigned by the language model to every text \mathbf{d} in the difference between implied exclusions $(\mathcal{X}_A \setminus \mathcal{X}_B)(\mathbf{x})$. Therefore, we make two key approximations to estimate $\hat{b}_{B\|A}(\mathbf{x}) \approx b_{B\|A}(\mathbf{x})$ (and analogously $\hat{b}_{A\|B}(\mathbf{x}) \approx b_{A\|B}(\mathbf{x})$) at nearly zero computational overhead.

Approximating $\mathcal{X}(T(\mathbf{x}))$ via $\mathcal{X}(T(\mathbf{x})_n)$. We approximate the implied exclusions of $T(\mathbf{x})$ via the implied exclusions of the last token $T(\mathbf{x})_n$ in $T(\mathbf{x})$.

$$\hat{\mathcal{X}}(T(\mathbf{x})) = \{D(T(\mathbf{x})_{<n}) \odot \mathbf{u} \mid \mathbf{u} \in \mathcal{X}(T(\mathbf{x})_n)\} \quad (\text{Bias Approx. 1})$$

This makes it possible to precompute the implied exclusions $\mathcal{X}(t)$ for all $t \in \mathcal{V}$.

Approximating $p(T(\mathbf{x}))$ via $p_{\text{unigram}}(T(\mathbf{x})_n)$. We approximate the language model likelihood $p(T(\mathbf{x}))$ via the unigram likelihood $p_{\text{unigram}}(T(\mathbf{x})_n)$ computed via the token counts of a text corpus.

$$\hat{p}(T(\mathbf{x})) = p_{\text{unigram}}(T(\mathbf{x})_n) \quad (\text{Bias Approx. 2})$$

This approximation is crude by necessity since it is distinctly intractable to run every token sequence $\mathbf{d} \in (\mathcal{X}_A \setminus \mathcal{X}_B)(\mathbf{x})$ through a large language model. However, we show later in Section 4 that it performs well in practice. Bias Approx. 1 and Bias Approx. 2 together make the bias only depend on the last token in the sequence. Going back to our distillation setup, the above approximations allow precomputing the bias difference $\hat{b}_{S,T}(\mathbf{x})$ for any text by enumerating all possible last token pairs $(t_S, t_T) \in \mathcal{V}_S \times \mathcal{V}_T$ and storing the result in a sparse matrix in $\mathbb{R}^{|\mathcal{V}_S| \times |\mathcal{V}_T|}$. This achieves our goal of defining an efficiently computable scalar metric to measure the difference in tokenization bias between two token sequences, and lets us set the alignment constraint to $c(\mathbf{y}, \mathbf{z}) := \max(\hat{b}_{S,T}(\mathbf{y}), \hat{b}_{S,T}(\mathbf{z})) \leq \gamma$ where γ is a manually defined bias difference threshold. We analyse the sensitivity to γ in Appendix B.4. In summary, our objective is based on minimising the likelihood difference between chunks of tokens with low differences in tokenization bias, i.e., chunks

which should have *approximately equal* likelihoods. To do so, we minimize a binarised f -divergence between the chunk likelihoods (Figure 2), enabling pure cross-tokenizer distillation for the first time.

3.2 Additional Considerations

Distilling Hidden States Across Tokenizers. A limitation of our method is that the teacher signal has lower information content than usual. Since we match chunk probabilities represented as 32-bit floating point numbers, the teacher signal has $|\mathcal{A}_c| \times 32$ bit per text, while it has $\mathcal{O}(|V|)$ more information at $|T(\mathbf{x})| \times |\mathcal{V}| \times 32$ bit in the standard setup when the teacher and the student have the same tokenizer (i.e., minimizing KL divergence between the teacher and the student next-token distributions). To make up for this relative sparsity of the signal, we optionally add an auxiliary loss maximizing the similarity of aligned hidden states between the teacher and the student.

$$\mathcal{L}_{S,T}^{\text{hidden}}(\mathbf{x}) = \sum_{l_T, l_S \in L_{T,S}} \sum_{i,j,k,l \in \mathbf{A}(\mathbf{x})} \|H_T(T_T(\mathbf{x}))_j^{l_T} - \text{proj}(H_S(T_S(\mathbf{x}))_i^{l_S})\|$$

(Hidden State Alignment Objective)

where $H_\star(\dots)_i^l$ are the language models’ hidden states at layer l and index i in the sequence and $L_{T,S} \in \mathbb{Z}^2$ are layer-wise alignments between the teacher and the student (e.g., indicating that the last layer hidden states of the two models should be aligned). $\text{proj}(\star) : \mathbb{R}^{d_S} \rightarrow \mathbb{R}^{d_T}$ is a learned projection function mapping the student hidden states to the teachers’ dimensionality. We use greedy alignments without the constraint on the difference in tokenization bias as the hidden state alignments $\mathbf{A}(\mathbf{x})$. The auxiliary loss enriches the signal from the teacher by $|\mathcal{A}| \times d_T \times 32$ bit. We find it to be particularly useful in some cases when the teacher and the student have the same underlying architecture (in case of *self-distillation*, c.f. Section 4).

Debiasing the Outcome Chunks. Note that there are two sources of bias in Chunk-Level Probability: the bias difference between the conditions $T(\mathbf{x})_{:i}$, as well as the bias difference between the outcome chunks $T(\mathbf{x})_{i:j}$. We observe that we can avoid the bias stemming from the outcome chunks. Specifically, we can modify the chunk-level probability to

$$p^{\text{debiased}}(\mathbf{x}, i:j) := p(T(\mathbf{x})_{i:j}|T(\mathbf{x})_{:i}) \cdot \sum \{p(t|T(\mathbf{x})_{:j}) \mid t \in \mathcal{V}, t \text{ starts with any } b \in \mathcal{B}\}$$

(Outcome-Debiased Chunk-Level Probability)

Here, \mathcal{B} is the set of pretoken-boundary bytes; these are bytes which never occur within a token (in practice, this can be e.g. whitespace such as the bytes corresponding to the `\n`, `\t` and the space character). This debiasing has been first introduced by Pimentel & Meister (2024) in the context of computing the conditional probability of words correctly (i.e., in an unbiased way). The effect of comparing the joint probability of the chunk tokens and the chunk being followed by a pretoken boundary is that we *explicitly* exclude all implied exclusions since the implied exclusions can never contain a pretoken-boundary byte. Thus, while the probabilities compared in Chunk-Level Probability could be biased by one of the two chunks implicitly excluding a token sequence with high likelihood, Outcome-Debiased Chunk-Level Probability avoids this issue. Appendix B.3 shows an example and ablates the empirical impact of outcome chunk debiasing.

4 Experiments

We experimentally verify our method on two distinct use cases. First, we observe that self-distillation across tokenizers enables an unprecedentedly effective transfer of a pre-trained language model to a different tokenizer, which we explore in Use Case 1. Secondly, we find that ALM improves over prior cross-tokenizer distillation objectives at distilling a large maths-specialized model into a much smaller model (Use Case 2). This is evidence toward the greatly expanded possible teacher–student combinations now enabled by ALM.

Use Case 1: Tokenizer Transfer via Self-Distillation

Tokenizer transfer is the problem of transferring a pretrained language model to a different tokenizer which typically has some desirable properties (c.f. Rust et al., 2021). We observe that tokenizer

Table 1: Results of transferring the Llama 3.2 3B IT and Gemma 2 2B IT LLMs to the Qwen2 tokenizer and to byte-level tokenization. *original* denotes the original model without transfer. *ARC-C* refers to Arc-Challenge. *AGI-EN* and *AGI-ZH* refer to the English and Chinese splits of AGIEval.

Model	Tokenizer Method	Benchmark								Avg.	
		PiQA	ARC-C	BoolQ	MMLU	Arith.	AGI-EN	AGI-ZH	IFEval		
Llama 3.2 3B IT	<i>original</i>	76.9	43.9	78.8	62.4	79.5	36.6	40.2	76.6	61.9	
	Qwen2	SFT	76.7	41.2	80.3	60.6	24.9	33.8	29.4	63.5	51.3
		DSKD	75.8	39.5	80.1	60.1	11.3	34.1	30.3	66.6	49.7
		MinED	76.8	40.9	80.3	60.7	34.3	34.1	30.2	65.4	52.8
		ALM + SFT	76.4	41.4	80.3	60.6	24.5	33.8	29.9	64.0	51.4
		ALM	77.1	43.6	78.9	61.8	50.3	36.6	33.2	76.0	57.2
	Byte	SFT	74.5	37.9	66.1	51.8	8.7	31.2	32.8	61.3	45.5
		DSKD	72.3	35.1	75.5	50.9	24.4	30.7	31.7	60.5	47.6
		MinED	74.6	36.4	78.7	50.9	10.8	32.1	30.8	60.8	46.9
		ALM + SFT	74.7	38.1	76.9	55.6	67.0	33.8	35.4	58.3	55.0
ALM		74.3	38.9	75.1	55.5	62.1	36.1	34.2	54.4	53.8	
Gemma 2 2B IT	<i>original</i>	79.6	50.4	83.8	56.9	84.8	42.1	30.7	62.5	61.4	
	Qwen2	SFT	76.1	42.2	77.3	50.0	18.5	31.6	29.0	56.6	47.7
		DSKD	76.2	42.8	79.5	51.4	62.5	33.4	28.4	57.3	53.9
		MinED	76.4	43.2	77.1	50.1	1.8	31.3	29.0	56.4	45.7
		ALM + SFT	76.2	42.4	77.7	50.3	40.4	31.7	28.9	54.2	50.2
		ALM	76.9	46.9	82.8	53.8	83.9	38.8	32.3	62.5	59.8
	Byte	SFT	70.0	31.8	65.6	40.9	24.6	24.5	26.9	45.1	41.2
		DSKD	70.3	32.4	67.0	43.9	49.3	25.8	26.9	45.4	45.1
		MinED	69.6	31.7	67.4	41.2	51.6	24.8	26.9	43.3	44.6
		ALM + SFT	70.1	36.1	81.0	44.9	66.1	26.7	26.9	39.8	49.0
ALM		69.7	35.3	80.1	45.4	66.7	26.5	26.9	40.3	48.9	

transfer can be treated as cross-tokenizer distillation: the teacher is the language model with the original tokenizer, and the student is the language model with the new tokenizer. This is an instance of *self-distillation* since the teacher and the student have the same backbone. We investigate two particular applications of tokenizer transfer via self-distillation. First, we transfer multiple language models to the same (subword) tokenizer; this enables token-level ensembling, improving their performance. Second, we transfer subword-based language models to the byte-level, which may be an attractive way of creating byte-level models instead of expensively training from scratch.

Models. We use the instruction-tuned Gemma2 2B IT (Gemma Team et al., 2024) and the instruction-tuned Llama 3.2 3B IT (Grattafiori et al., 2024) as the models for self-distillation. We transfer these models to the Qwen2 tokenizer; this enables ensembling the models with models of the Qwen series, for which we choose Qwen2.5 1.5B IT (Qwen et al., 2025).

Baseline Methods. We compare against the current standard methodology for tokenizer transfer, which consists of initializing the new token embeddings using a heuristic (e.g. Tran, 2020; Minixhofer et al., 2022; Gee et al., 2022; Dobler & de Melo, 2023), then training on next-token prediction; we refer to this baseline as *SFT*. We use FVT (Gee et al., 2022) as the initialization heuristic due to its conceptual simplicity and competitive performance with more complex methods (c.f. Minixhofer et al., 2024). We also analyse how well existing methods for cross-tokenizer distillation perform in our novel tokenizer transfer self-distillation setup. Here, we choose the DSKD Zhang et al. (2024) and MinED (Wan et al., 2024) methods.⁹ Importantly, DSKD and MinED auxilarily add cross-tokenizer distillation to the primary next-token prediction objective, so they necessarily need to train jointly on next-token prediction and distillation; this is not the case for our ALM method. We thus also experiment with *ALM + SFT*, which is our objective plus next-token prediction.

Training. We train on the Tulu3 instruction-tuning dataset (Lambert et al., 2025) with a batch size of 64 texts and a sequence length of 512 tokens for both student and teacher. We use the Adam

⁹We forgo comparison against ULD (Boizard et al., 2025) since DSKD and MinED have been shown to perform consistently better by Wan et al. (2024) and Zhang et al. (2024).

Table 2: Results of ensembling the Gemma 2 2B IT and Llama 3.2 3B IT models transferred to the Qwen tokenizer with Qwen2.5 1.5B IT. The ensemble outperforms its parts and their original version (before tokenizer transfer), increasing performance to within the range of substantially larger models.

Size Model		Benchmark								Avg.
		PiQA	ARC-C	BoolQ	MMLU	Arith.	AGI-EN	AGI-ZH	IFEval	
Original Models	2.6B Gemma2 2B IT	79.6	50.4	83.8	56.9	84.8	42.1	30.7	62.5	61.4
	3.2B Llama3.2 3B IT	76.9	43.9	78.8	62.4	79.5	36.6	40.2	76.6	61.9
Ensemble Constituents	1.5B Qwen2.5 1.5B IT	76.3	43.2	77.9	60.1	0.8	45.0	54.2	46.3	50.5
	2.4B Gemma 2 2B IT \rightarrow Q Tok.	76.9	46.9	82.8	53.8	83.9	38.8	32.3	62.5	59.8
	3.3B Llama 3.2 3B IT \rightarrow Q Tok.	77.1	43.6	78.9	61.8	50.3	36.6	33.2	76.0	57.2
Ensemble	7.2B Q+G+L (Mean Prob.)	77.7	46.7	83.6	62.9	81.4	44.1	45.9	64.6	63.4
	7.2B Q+G+L (Mean Logits)	77.7	47.3	84.2	62.3	70.0	44.3	48.3	67.8	62.7
Larger Models	7.6B Qwen2.5 7B IT	80.4	54.3	86.4	71.7	1.9	57.6	72.6	76.6	62.7
	8.0B Llama3.1 8B IT	81.6	53.9	85.4	68.4	86.6	47.3	47.1	81.7	69.0

optimizer (Kingma & Ba, 2015) following the adaptation settings of Groeneveld et al. (2024). For methods combining distillation with SFT, an important hyperparameter is the distillation coefficient β modulating the contribution of the distillation objective via $\mathcal{L}^{\text{total}} = \mathcal{L}^{\text{SFT}} + \beta \cdot \mathcal{L}^{\text{distil}}$. We sweep over the learning rate and β separately for every baseline method (results in Appendix B.1), choosing a learning rate of $1e-5$ and distillation coefficient $\beta = 1$. We train for 20k steps and linearly warm up the learning rate to its peak over the first 2k steps, then linearly anneal to zero. We use LoRA (Hu et al., 2022) with $\alpha = r = 64$; this enables substantial memory savings (c.f. Section 5). For ALM, we use a bias threshold $\gamma = 1e-4$ and analyze the sensitivity to this hyperparameter in Appendix B.4. Furthermore, we add an embedding projector to project the (FVT-initialized) embeddings. This allows learning a single set of shared parameters projecting from the original tokenizers’ embedding space to the new embedding space, instead of purely learning to update every embedding individually; see Appendix B.3 for details on this component. The training setup is the same for all methods.

Adjustments for Transfer to Bytes. For the transfer to bytes, we quadruple the student sequence length to 2048,¹⁰ halve the batch size to 32 texts, increase the learning rate to $3e-5$, train the full model and do not add an embedding projector. Adding the hidden state distillation loss leads to consistent improvements (while results are mixed in the subword case), so we add it here and do not add it for subword-to-subword transfer. We also untie the embedding matrices since sharing the input and output embedding parameters has negligible impact on the parameter count when the vocabulary just consists of the 255 possible bytes. Transfer to bytes substantially decreases the parameter count due to shrinking the embedding matrix (which can make up a considerable portion of the total parameters). Thus, to make it less destructive, we devise a strategy to re-incorporate the subword embedding parameters: for every byte position, we backtrack to find the longest matching subword token ending at this position. We then add the embedding of this token to the byte embedding. This is akin to BLT’s strategy of adding n-gram embeddings Pagnoni et al. (2024), where in our case the vocabulary is given by the subword-based model. This strategy only accounts for the parameter mismatch at the *input layer*, not at the output layer, so we might still expect decreased performance. As a final modification, we also find it beneficial to use an ALM loss with chunks spanning from whitespace to whitespace in addition to the primary ALM loss; this is possibly due to the chunk debiasing (c.f. Section 3.2) being more robust in this case since the chunks are closer to words (and the pretoken-boundary probability is thus higher on average), which provides a useful auxiliary signal.¹¹ Future work could investigate the behaviour of different chunking strategies more thoroughly.

Evaluation & Results. We evaluate on a standard set of natural language benchmarks consisting of PiQA (Bisk et al., 2020), ARC-Challenge (Clark et al., 2018), BoolQ (Clark et al., 2019), MMLU (Hendrycks et al., 2021), one to five digit arithmetic as evaluated by Brown et al. (2020),

¹⁰The increase in sequence length is necessary since one token consists of ≈ 4 bytes on average. The other hyperparameters were found in preliminary experiments.

¹¹We do not experiment with this chunking strategy as the primary objective since it does not generalise to languages which do not use whitespace to separate words (e.g. Chinese and Thai).

AGIEval (Zhong et al., 2023)¹² and IFEval (Zhou et al., 2023). We use `lm-eval` (Gao et al., 2024) for all evaluations. Table 1 shows tokenizer transfer results. In the first application, transfer to the subword-level Qwen2 tokenizer, ALM vastly outperforms all non-pure distillation objectives (including ALM + SFT) and enables largely retaining the original models’ performance. In particular, on arithmetic (which might be under-represented in the training data), SFT-based methods seem to suffer from catastrophic forgetting, while ALM comes closest to retaining performance.¹³ In the byte-transfer case, ALM + SFT slightly outperforms ALM, with both of them vastly outperforming SFT and all prior distillation methods. In fact, transferring Llama 3.2 3B IT to bytes via ALM is more effective than transferring the model to the (similar) Qwen2 subword tokenizer using prior methods. ALM + SFT may outperform ALM here since naïve transfer to bytes is necessarily strongly destructive since the model has to adapt to a vastly different granularity, so preserving the original model’s behaviour is less crucial. In both cases, a gap with respect to the original model remains. There are multiple avenues toward closing this gap: it may be beneficial to add an additional distillation phase on pretraining data (whereas we only do instruction-tuning), to add more layers to close the gap in effective parameter count, to retrofit the model into an hourglass architecture with token merging as in e.g. DTP (Nawrot et al., 2023) or BLT (Pagnoni et al., 2024), and/or to add multi-byte prediction (Gloeckle et al., 2024). Table 2 shows the results of ensembling the Llama, Gemma and Qwen models. To our knowledge, this is the first ensemble of LLMs with different tokenizers without severe methodological restrictions.¹⁴ The ensemble improves over its constituents due to two characteristics: (i) on tasks where all constituents perform at a similar level, the ensemble improves over the performance of each individual model (e.g., PiQA, Arc-c, BoolQ, MMLU) and (ii) on tasks where either one of the constituents performs exceptionally well, the ensemble moves the needle toward this level of performance, although it doesn’t reach it (e.g., Arithmetic, AGIEval-EN, AGIEval-ZH, IFEval). Our ensemble improves upon its constituents via naïvely averaging the models’ logits or predicted probabilities. We believe these results open the door toward better inter-model combination via more sophisticated ensembling (e.g., Ormazabal et al., 2023), routing (e.g., Shen et al., 2024) and/or merging (e.g., Sharma et al., 2024).

Use Case 2: Large-to-Small Distillation Across Tokenizers

To investigate the efficacy of our method in a large-to-small distillation setting, we scale up from the evaluation setups used in prior work on cross-tokenizer distillation to a realistic larger-scale setup: distilling the maths-specialized OpenMath2-Llama3.1-8B (Toshniwal et al., 2024) into Gemma2 2B.

Baselines. As in Use Case 1, we compare our method against training with SFT, DSKD, and MinED. We additionally report scores of the teacher as an upper bound on performance and of general-purpose instruction-tuned Gemma2 2B IT as a lower bound on performance.

Training. We use the OpenMathInstruct-2 dataset (which the teacher has been trained on; Toshniwal et al., 2024) as the distillation training data and follow the training setup from Use Case 1, apart from the following adjustments. We increase the sequence length to 1024 to allow for longer chain-of-thought traces and double the batch size to 64. We accordingly reduce the training steps to 5k to train for an equivalent total amount of tokens. We also found it beneficial to train the full model and reduce the learning rate to $5e-6$ in preliminary experiments.

Evaluation & Results. We evaluate zero-shot accuracy on GSM8K (Cobbe et al., 2021) and the MATH benchmark (Hendrycks et al., 2021) following Toshniwal et al. (2024). Table 3 shows the results. Notably, the SFT baseline is competitive, as evidenced by MinED and DSKD not consistently surpassing it. However, ALM + SFT does consistently surpass SFT, leading to an improvement of

¹²For AGIEval, we report the macro-average over the English and Chinese subsets excluding GaoKao Math Cloze and AGIEval Math since they are not designed for instruction-tuned models in their published form.

¹³Retaining arithmetic performance is especially challenging for transfer from the Llama3 tokenizer to the Qwen2 tokenizer since Llama3 has tokens for numbers with up to 3 digits while in Qwen2 every digit is a separate token. The model thus has to adjust its understanding of numbers without large dedicated amounts of training data. Automatically detecting & fixing underperformance of an adapted (e.g., tokenizer-transferred) model on specific domains may be a promising direction for future work (see also Albalak et al., 2024).

¹⁴Prior work ensembled LLMs with different tokenizers by sampling at the byte-level (which requires a specialized sampling procedure and results in additional overhead; Phan et al., 2024) or combining their sequence-level likelihoods (which makes generation impossible; Mavromatis et al., 2024).

Table 3: Results of cross-tokenizer distilling the large math-specialized OpenMath2-Llama3.1-8B into the small Gemma2 2B language model. All results are zero-shot CoT.

Model	Method	GSM8K	MATH	Avg.
OpenMath2-Llama3.1-8B (Teacher)		88.9	60.2	74.6
Gemma2 2B IT		6.1	11.3	8.7
Gemma2 2B	SFT	62.9	32.5	47.7
	DSKD	62.5	31.6	47.1
	MinED	64.2	32.2	48.2
	ALM + SFT	65.1	32.9	49.0
	ALM	61.5	27.6	44.6

Table 4: Required TFLOPS and Memory per TensorCore of a TPU v3-8 for processing a batch of size 8 (forward + backward pass) when transferring Gemma 2 2B IT to the Qwen tokenizer.

	SFT	DSKD	MinED	ALM	ALM + SFT
TFLOPS	10.6	15.5 (+46%)	13.4 (+26%)	13.3 (+25%)	13.3 (+25%)
Memory (GB)	5.8	8.0 (+37%)	10.4 (+79%)	6.1 (+5%)	6.4 (+10%)

1.3% points on average while greatly surpassing the general-purpose Gemma2 2B IT and achieving 49.0 / 74.6 of the teachers’ performance at 4x fewer parameters.

5 Discussion

How Substantial Is the Overhead from Distillation? We report the TFLOPS and Memory requirements of the different distillation methods and the SFT baseline in Table 4. This serves as an approximate way to quantify the computational overhead required for training a model with any given method.¹⁵ DSKD requires substantially more TFLOPs than the other methods since there is an extra cross-attention step between the teacher and the student sequences which can incur substantial costs. This is further exacerbated with longer contexts (e.g., when transferring to bytes). MinED needs substantially more memory since the $|T(\mathbf{x})| \times |V|$ matrix of logits needs to be aligned with the student along the sequence *and* vocabulary dimensions, as well as renormalized via a softmax. ALM suffers from neither of these constraints. Additionally, although distillation leads to a $\approx 25\%$ TFLOPS overhead, in the self-distillation case the memory overhead can be mitigated via Parameter Efficient Fine-Tuning (PEFT) methods (in our case LoRA; c.f. Pfeiffer et al., 2023). Here, PEFT enables storing only a single copy of the full model parameters to propagate through both the teacher and the student since they remain unchanged (only some additional PEFT parameters are updated).

6 Conclusion

We have introduced ALM, a cross-tokenizer distillation method which has enabled pure distillation across tokenizers for the first time. ALM leads to substantial and consistent improvements over prior methods as demonstrated in experiments on a novel viewpoint of tokenizer transfer as self-distillation (Use Case 1) as well as large-to-small distillation across tokenizers (Use Case 2). This has enabled, for example, (i) creating effective byte-level models at a fraction of the cost of training from scratch by transferring a pretrained (subword-level) model to bytes via cross-tokenizer self-distillation with ALM, (ii) transferring multiple different models to the same tokenizer to boost their performance via ensembling and (iii) distilling a large maths-specialized model into a smaller model with a different tokenizer. Our work provides a foundation for further enhancements, such as retrofitting into dedicated byte-level architectures for (i) and more sophisticated combinations via ensembling/routing/merging for (ii). In aggregate, ALM takes substantial strides toward vastly expanding the possible combinations of teacher–student pairs for distillation and utilising new applications for transferring knowledge across diverse language models.

¹⁵These numbers may vary depending on the implementation; we predominantly follow the existing public implementations of DSKD and MinED. We do not implement dedicated optimizations for any method (including ours). However, we expect the observed trends to be consistent.

7 Limitations

While our method substantially and consistently outperforms prior work, there are inconsistencies in which variant of our method performs best (ALM for transfer to another subword-level tokenizer, ALM + SFT for transfer to the byte-level and large-to-small distillation). Adapting the distillation coefficient β or more sophisticated loss combination methods such as GradNorm (Chen et al., 2018) could shed more light on this dynamic; due to resource constraints, we have not investigated these. Furthermore, we have restricted our experiments to models ranging from 2.4B to 3.3B parameters. It is not yet clear how well ALM scales to models with higher parameter counts. Finally, we have observed on transfer to the byte-level that adding an auxiliary loss based on chunks spanning from whitespace to whitespace improves performance, highlighting the necessity for future work to more thoroughly explore the solution space of chunking methods for ALM.

Acknowledgments

This work has been supported by a Royal Society University Research Fellowship ‘*Inclusive and Sustainable Language Technology for a Truly Multilingual World*’ (no 221137; 2022-) awarded to Ivan Vulić. Research supported by the Google Cloud Research Credits program with the award GCP329647813. Research supported with Cloud TPUs from Google’s TPU Research Cloud (TRC). We would like to thank Andreas Grivas, Giwon Hong and Hannah Sterz for their helpful feedback on the paper draft.

References

- Alon Albalak, Yanai Elazar, Sang Michael Xie, Shayne Longpre, Nathan Lambert, Xinyi Wang, Niklas Muennighoff, Bairu Hou, Liangming Pan, Haewon Jeong, Colin Raffel, Shiyu Chang, Tatsunori Hashimoto, and William Yang Wang. A survey on data selection for language models. *Transactions on Machine Learning Research*, 2024. ISSN 2835-8856. URL <https://openreview.net/forum?id=XfHWcNTSHp>. Survey Certification.
- Yonatan Bisk, Rowan Zellers, Ronan Le Bras, Jianfeng Gao, and Yejin Choi. PIQA: Reasoning about Physical Commonsense in Natural Language. In *Thirty-Fourth AAAI Conference on Artificial Intelligence*, 2020.
- Nicolas Boizard, Kevin El Haddad, Celine Hudelot, and Pierre Colombo. Towards cross-tokenizer distillation: the universal logit distillation loss for LLMs. *Transactions on Machine Learning Research*, 2025. ISSN 2835-8856. URL <https://openreview.net/forum?id=bwRxXiG09A>.
- Tom Brown, Benjamin Mann, Nick Ryder, Melanie Subbiah, Jared D Kaplan, Prafulla Dhariwal, Arvind Neelakantan, Pranav Shyam, Girish Sastry, Amanda Askell, Sandhini Agarwal, Ariel Herbert-Voss, Gretchen Krueger, Tom Henighan, Rewon Child, Aditya Ramesh, Daniel Ziegler, Jeffrey Wu, Clemens Winter, Chris Hesse, Mark Chen, Eric Sigler, Mateusz Litwin, Scott Gray, Benjamin Chess, Jack Clark, Christopher Berner, Sam McCandlish, Alec Radford, Ilya Sutskever, and Dario Amodei. Language models are few-shot learners. In H. Larochelle, M. Ranzato, R. Hadsell, M.F. Balcan, and H. Lin (eds.), *Advances in Neural Information Processing Systems*, volume 33, pp. 1877–1901. Curran Associates, Inc., 2020. URL https://proceedings.neurips.cc/paper_files/paper/2020/file/1457c0d6bfc4967418bfb8ac142f64a-Paper.pdf.
- Cristian Bucilua, Rich Caruana, and Alexandru Niculescu-Mizil. Model compression. In *Proceedings of the 12th ACM SIGKDD international conference on Knowledge discovery and data mining, KDD ’06*, pp. 535–541, New York, NY, USA, August 2006. Association for Computing Machinery. ISBN 978-1-59593-339-3. doi: 10.1145/1150402.1150464. URL <https://dl.acm.org/doi/10.1145/1150402.1150464>.
- Dan Busbridge, Amitis Shidani, Floris Weers, Jason Ramapuram, Etai Littwin, and Russ Webb. Distillation Scaling Laws, February 2025. URL <http://arxiv.org/abs/2502.08606>. arXiv:2502.08606 [cs].
- Zhao Chen, Vijay Badrinarayanan, Chen-Yu Lee, and Andrew Rabinovich. Gradnorm: Gradient normalization for adaptive loss balancing in deep multitask networks. In *International conference on machine learning*, pp. 794–803. PMLR, 2018.
- Christopher Clark, Kenton Lee, Ming-Wei Chang, Tom Kwiatkowski, Michael Collins, and Kristina Toutanova. BoolQ: Exploring the Surprising Difficulty of Natural Yes/No Questions. In Jill Burstein, Christy Doran, and Thamar Solorio (eds.), *Proceedings of the 2019 Conference of the North American Chapter of the Association for Computational Linguistics: Human Language Technologies, Volume 1 (Long and Short Papers)*, pp. 2924–2936, Minneapolis, Minnesota, June 2019. Association for Computational Linguistics. doi: 10.18653/v1/N19-1300. URL <https://aclanthology.org/N19-1300>.

- Peter Clark, Isaac Cowhey, Oren Etzioni, Tushar Khot, Ashish Sabharwal, Carissa Schoenick, and Oyvind Tafjord. Think you have solved question answering? try arc, the ai2 reasoning challenge. *arXiv:1803.05457v1*, 2018.
- Karl Cobbe, Vineet Kosaraju, Mohammad Bavarian, Mark Chen, Heewoo Jun, Lukasz Kaiser, Matthias Plappert, Jerry Tworek, Jacob Hilton, Reiichiro Nakano, Christopher Hesse, and John Schulman. Training verifiers to solve math word problems. *arXiv preprint arXiv:2110.14168*, 2021.
- Jacob Devlin, Ming-Wei Chang, Kenton Lee, and Kristina Toutanova. BERT: Pre-training of Deep Bidirectional Transformers for Language Understanding. *arXiv:1810.04805 [cs]*, May 2019. URL <http://arxiv.org/abs/1810.04805>. arXiv: 1810.04805.
- Konstantin Dobler and Gerard de Melo. FOCUS: Effective Embedding Initialization for Monolingual Specialization of Multilingual Models. In Houda Bouamor, Juan Pino, and Kalika Bali (eds.), *Proceedings of the 2023 Conference on Empirical Methods in Natural Language Processing*, pp. 13440–13454, Singapore, December 2023. Association for Computational Linguistics. doi: 10.18653/v1/2023.emnlp-main.829. URL <https://aclanthology.org/2023.emnlp-main.829>.
- Darius Feher, Ivan Vulić, and Benjamin Minixhofer. Retrofitting large language models with dynamic tokenization, 2024. URL <https://arxiv.org/abs/2411.18553>.
- Yao Fu, Hao Peng, Litu Ou, Ashish Sabharwal, and Tushar Khot. Specializing smaller language models towards multi-step reasoning. In Andreas Krause, Emma Brunskill, Kyunghyun Cho, Barbara Engelhardt, Sivan Sabato, and Jonathan Scarlett (eds.), *Proceedings of the 40th International Conference on Machine Learning*, volume 202 of *Proceedings of Machine Learning Research*, pp. 10421–10430. PMLR, 23–29 Jul 2023. URL <https://proceedings.mlr.press/v202/fu23d.html>.
- Leo Gao, Jonathan Tow, Baber Abbasi, Stella Biderman, Sid Black, Anthony DiPofi, Charles Foster, Laurence Golding, Jeffrey Hsu, Alain Le Noac’h, Haonan Li, Kyle McDonell, Niklas Muennighoff, Chris Ociepa, Jason Phang, Laria Reynolds, Hailey Schoelkopf, Aviya Skowron, Lintang Sutawika, Eric Tang, Anish Thite, Ben Wang, Kevin Wang, and Andy Zou. A framework for few-shot language model evaluation, 07 2024. URL <https://zenodo.org/records/12608602>.
- Leonidas Gee, Andrea Zugarini, Leonardo Rigutini, and Paolo Torrioni. Fast Vocabulary Transfer for Language Model Compression. In Yunyao Li and Angeliki Lazaridou (eds.), *Proceedings of the 2022 Conference on Empirical Methods in Natural Language Processing: Industry Track*, pp. 409–416, Abu Dhabi, UAE, December 2022. Association for Computational Linguistics. doi: 10.18653/v1/2022.emnlp-industry.41. URL <https://aclanthology.org/2022.emnlp-industry.41>.
- Gemma Team, Morgane Riviere, Shreya Pathak, Pier Giuseppe Sessa, Cassidy Hardin, et al. Gemma 2: Improving open language models at a practical size, 2024. URL <https://arxiv.org/abs/2408.00118>.
- Fabian Gloeckle, Badr Youbi Idrissi, Baptiste Roziere, David Lopez-Paz, and Gabriel Synnaeve. Better & faster large language models via multi-token prediction. In *Forty-first International Conference on Machine Learning*, 2024. URL <https://openreview.net/forum?id=pEWAcEjiU2>.
- Aaron Grattafiori, Abhimanyu Dubey, Abhinav Jauhri, Abhinav Pandey, Abhishek Kadian, et al. The llama 3 herd of models, 2024. URL <https://arxiv.org/abs/2407.21783>.
- Dirk Groeneveld, Iz Beltagy, Evan Walsh, Akshita Bhagia, Rodney Kinney, Oyvind Tafjord, Ananya Jha, Hamish Ivison, Ian Magnusson, Yizhong Wang, Shane Arora, David Atkinson, Russell Authur, Khyathi Chandu, Arman Cohan, Jennifer Dumas, Yanai Elazar, Yuling Gu, Jack Hessel, Tushar Khot, William Merrill, Jacob Morrison, Niklas Muennighoff, Aakanksha Naik, Crystal Nam, Matthew Peters, Valentina Pyatkin, Abhilasha Ravichander, Dustin Schwenk, Saurabh Shah, William Smith, Emma Strubell, Nishant Subramani, Mitchell Wortsman, Pradeep Dasigi, Nathan Lambert, Kyle Richardson, Luke Zettlemoyer, Jesse Dodge, Kyle Lo, Luca Soldaini, Noah Smith, and Hannaneh Hajishirzi. OLMo: Accelerating the science of language models. In Lun-Wei Ku, Andre Martins, and Vivek Srikumar (eds.), *Proceedings of the 62nd Annual Meeting of the Association for Computational Linguistics (Volume 1: Long Papers)*, pp. 15789–15809, Bangkok, Thailand, August 2024. Association for Computational Linguistics. doi: 10.18653/v1/2024.acl-long.841. URL <https://aclanthology.org/2024.acl-long.841/>.
- Yuxian Gu, Li Dong, Furu Wei, and Minlie Huang. MiniLLM: Knowledge distillation of large language models. In *The Twelfth International Conference on Learning Representations*, 2024. URL <https://openreview.net/forum?id=5h0qf71BZZ>.
- Dan Hendrycks, Collin Burns, Saurav Kadavath, Akul Arora, Steven Basart, Eric Tang, Dawn Song, and Jacob Steinhardt. Measuring mathematical problem solving with the MATH dataset. In *Thirty-fifth Conference on Neural Information Processing Systems Datasets and Benchmarks Track (Round 2)*, 2021. URL <https://openreview.net/forum?id=7Bywt2mQsCe>.

- Geoffrey Hinton, Oriol Vinyals, and Jeff Dean. Distilling the Knowledge in a Neural Network, March 2015. URL <http://arxiv.org/abs/1503.02531>. arXiv:1503.02531 [stat].
- Edward J Hu, yelong shen, Phillip Wallis, Zeyuan Allen-Zhu, Yuanzhi Li, Shean Wang, Lu Wang, and Weizhu Chen. LoRA: Low-rank adaptation of large language models. In *International Conference on Learning Representations*, 2022. URL <https://openreview.net/forum?id=nZeVKeeFYf9>.
- Leonid V Kantorovich. Mathematical methods of organizing and planning production. *Management science*, 6(4):366–422, 1960.
- Diederik P. Kingma and Jimmy Ba. Adam: A method for stochastic optimization. In Yoshua Bengio and Yann LeCun (eds.), *3rd International Conference on Learning Representations, ICLR 2015, San Diego, CA, USA, May 7-9, 2015, Conference Track Proceedings*, 2015. URL <http://arxiv.org/abs/1412.6980>.
- Jongwoo Ko, Sungnyun Kim, Tianyi Chen, and Se-Young Yun. DistiLLM: Towards streamlined distillation for large language models. In *Forty-first International Conference on Machine Learning*, 2024. URL <https://openreview.net/forum?id=lsHZNN0C7r>.
- Taku Kudo and John Richardson. SentencePiece: A simple and language independent subword tokenizer and detokenizer for Neural Text Processing. In Eduardo Blanco and Wei Lu (eds.), *Proceedings of the 2018 Conference on Empirical Methods in Natural Language Processing: System Demonstrations*, pp. 66–71, Brussels, Belgium, November 2018. Association for Computational Linguistics. doi: 10.18653/v1/D18-2012. URL <https://aclanthology.org/D18-2012>.
- Solomon Kullback and Richard A Leibler. On information and sufficiency. *The annals of mathematical statistics*, 22(1):79–86, 1951.
- Nathan Lambert, Jacob Morrison, Valentina Pyatkin, Shengyi Huang, Hamish Ivison, Faeze Brahman, Lester James V. Miranda, Alisa Liu, Nouha Dziri, Shane Lyu, Yuling Gu, Saumya Malik, Victoria Graf, Jena D. Hwang, Jiangjiang Yang, Ronan Le Bras, Oyvind Tafjord, Chris Wilhelm, Luca Soldaini, Noah A. Smith, Yizhong Wang, Pradeep Dasigi, and Hannaneh Hajishirzi. Tulu 3: Pushing frontiers in open language model post-training, 2025. URL <https://arxiv.org/abs/2411.15124>.
- VI Levenshtein. Binary codes capable of correcting deletions, insertions, and reversals. *Proceedings of the Soviet physics doklady*, 1966.
- Costas Mavromatis, Petros Karypis, and George Karypis. Pack of llms: Model fusion at test-time via perplexity optimization, 2024. URL <https://arxiv.org/abs/2404.11531>.
- Benjamin Minixhofer, Fabian Paischer, and Navid Rekabsaz. WECHSEL: Effective initialization of subword embeddings for cross-lingual transfer of monolingual language models. Technical Report arXiv:2112.06598, arXiv, May 2022. URL <http://arxiv.org/abs/2112.06598>. arXiv:2112.06598 [cs] type: article.
- Benjamin Minixhofer, Edoardo Maria Ponti, and Ivan Vulić. Zero-shot tokenizer transfer, 2024. URL <https://arxiv.org/abs/2405.07883>.
- Piotr Nawrot, Jan Chorowski, Adrian Lancucki, and Edoardo Maria Ponti. Efficient Transformers with Dynamic Token Pooling. In Anna Rogers, Jordan Boyd-Graber, and Naoaki Okazaki (eds.), *Proceedings of the 61st Annual Meeting of the Association for Computational Linguistics (Volume 1: Long Papers)*, pp. 6403–6417, Toronto, Canada, July 2023. Association for Computational Linguistics. doi: 10.18653/v1/2023.acl-long.353. URL <https://aclanthology.org/2023.acl-long.353>.
- Saul B Needleman and Christian D Wunsch. A general method applicable to the search for similarities in the amino acid sequence of two proteins. *Journal of molecular biology*, 48(3):443–453, 1970.
- Aitor Ormazabal, Mikel Artetxe, and Eneko Agirre. CombLM: Adapting black-box language models through small fine-tuned models. In Houda Bouamor, Juan Pino, and Kalika Bali (eds.), *Proceedings of the 2023 Conference on Empirical Methods in Natural Language Processing*, pp. 2961–2974, Singapore, December 2023. Association for Computational Linguistics. doi: 10.18653/v1/2023.emnlp-main.180. URL <https://aclanthology.org/2023.emnlp-main.180/>.
- Artidoro Pagnoni, Ram Pasunuru, Pedro Rodriguez, John Nguyen, Benjamin Muller, Margaret Li, Chunting Zhou, Lili Yu, Jason Weston, Luke Zettlemoyer, Gargi Ghosh, Mike Lewis, Ari Holtzman, and Srinivasan Iyer. Byte Latent Transformer: Patches Scale Better Than Tokens, December 2024. URL <http://arxiv.org/abs/2412.09871>. arXiv:2412.09871 [cs].
- Jonas Pfeiffer, Sebastian Ruder, Ivan Vulić, and Edoardo Ponti. Modular deep learning. *Transactions on Machine Learning Research*, 2023. ISSN 2835-8856. URL <https://openreview.net/forum?id=z9EkXfvxta>. Survey Certification.

- Buu Phan, Brandon Amos, Itai Gat, Marton Havasi, Matthew Muckley, and Karen Ullrich. Exact Byte-Level Probabilities from Tokenized Language Models for FIM-Tasks and Model Ensembles, October 2024. URL <http://arxiv.org/abs/2410.09303>. arXiv:2410.09303 [cs].
- Tiago Pimentel and Clara Meister. How to compute the probability of a word. In Yaser Al-Onaizan, Mohit Bansal, and Yun-Nung Chen (eds.), *Proceedings of the 2024 Conference on Empirical Methods in Natural Language Processing*, pp. 18358–18375, Miami, Florida, USA, November 2024. Association for Computational Linguistics. doi: 10.18653/v1/2024.emnlp-main.1020. URL <https://aclanthology.org/2024.emnlp-main.1020/>.
- Qwen, ., An Yang, Baosong Yang, Beichen Zhang, Binyuan Hui, Bo Zheng, Bowen Yu, Chengyuan Li, Dayiheng Liu, Fei Huang, Haoran Wei, Huan Lin, Jian Yang, Jianhong Tu, Jianwei Zhang, Jianxin Yang, Jiayi Yang, Jingren Zhou, Junyang Lin, Kai Dang, Keming Lu, Keqin Bao, Kexin Yang, Le Yu, Mei Li, Mingfeng Xue, Pei Zhang, Qin Zhu, Rui Men, Runji Lin, Tianhao Li, Tianyi Tang, Tingyu Xia, Xingzhang Ren, Xuancheng Ren, Yang Fan, Yang Su, Yichang Zhang, Yu Wan, Yuqiong Liu, Zeyu Cui, Zhenru Zhang, and Zihan Qiu. Qwen2.5 technical report, 2025. URL <https://arxiv.org/abs/2412.15115>.
- Colin Raffel. Building machine learning models like open source software. *Communications of the ACM*, 66(2): 38–40, 2023.
- Alfréd Rényi. On measures of entropy and information. In *Proceedings of the fourth Berkeley symposium on mathematical statistics and probability, volume 1: contributions to the theory of statistics*, volume 4, pp. 547–562. University of California Press, 1961.
- Phillip Rust, Jonas Pfeiffer, Ivan Vulić, Sebastian Ruder, and Iryna Gurevych. How Good is Your Tokenizer? On the Monolingual Performance of Multilingual Language Models. *arXiv:2012.15613 [cs]*, June 2021. URL <http://arxiv.org/abs/2012.15613>. arXiv: 2012.15613.
- Rico Sennrich, Barry Haddow, and Alexandra Birch. Neural Machine Translation of Rare Words with Subword Units. In Katrin Erk and Noah A. Smith (eds.), *Proceedings of the 54th Annual Meeting of the Association for Computational Linguistics (Volume 1: Long Papers)*, pp. 1715–1725, Berlin, Germany, August 2016. Association for Computational Linguistics. doi: 10.18653/v1/P16-1162. URL <https://aclanthology.org/P16-1162>.
- Ekansh Sharma, Daniel M. Roy, and Gintare Karolina Dziugaite. The non-local model merging problem: Permutation symmetries and variance collapse, 2024. URL <https://arxiv.org/abs/2410.12766>.
- Zejiang Shen, Hunter Lang, Bailin Wang, Yoon Kim, and David Sontag. Learning to decode collaboratively with multiple language models. In Lun-Wei Ku, Andre Martins, and Vivek Srikumar (eds.), *Proceedings of the 62nd Annual Meeting of the Association for Computational Linguistics (Volume 1: Long Papers)*, pp. 12974–12990, Bangkok, Thailand, August 2024. Association for Computational Linguistics. doi: 10.18653/v1/2024.acl-long.701. URL <https://aclanthology.org/2024.acl-long.701/>.
- Yi Tay, Vinh Q. Tran, Sebastian Ruder, Jai Gupta, Hyung Won Chung, Dara Bahri, Zhen Qin, Simon Baumgartner, Cong Yu, and Donald Metzler. Charformer: Fast Character Transformers via Gradient-based Subword Tokenization. In *International Conference on Learning Representations*, 2022. URL <https://openreview.net/forum?id=JtBRnr10EFN>.
- Daniil Tiapkin, Daniele Calandriello, Johan Ferret, Sarah Perrin, Nino Vieillard, Alexandre Ramé, and Mathieu Blondel. On Teacher Hacking in Language Model Distillation, February 2025. URL <http://arxiv.org/abs/2502.02671>. arXiv:2502.02671 [cs].
- Shubham Toshniwal, Wei Du, Ivan Moshkov, Branislav Kisacanin, Alexan Ayrapetyan, and Igor Gitman. Openmathinstruct-2: Accelerating ai for math with massive open-source instruction data. *arXiv preprint arXiv:2410.01560*, 2024.
- Ke Tran. From English To Foreign Languages: Transferring Pre-trained Language Models. Technical Report arXiv:2002.07306, arXiv, April 2020. URL <http://arxiv.org/abs/2002.07306>. arXiv:2002.07306 [cs] type: article.
- Omri Uzan, Craig W. Schmidt, Chris Tanner, and Yuval Pinter. Greed is All You Need: An Evaluation of Tokenizer Inference Methods, 2024. [eprint: 2403.01289](https://arxiv.org/abs/2403.01289).
- Tim Vieira, Ben LeBrun, Mario Giulianelli, Juan Luis Gastaldi, Brian DuSell, John Terilla, Timothy J. O’Donnell, and Ryan Cotterell. From Language Models over Tokens to Language Models over Characters, December 2024. URL <http://arxiv.org/abs/2412.03719>. arXiv:2412.03719 [cs].

Fanqi Wan, Xinting Huang, Deng Cai, Xiaojun Quan, Wei Bi, and Shuming Shi. Knowledge fusion of large language models. In *The Twelfth International Conference on Learning Representations*, 2024. URL <https://openreview.net/forum?id=jiDsk12qcz>.

Linting Xue, Aditya Barua, Noah Constant, Rami Al-Rfou, Sharan Narang, Mihir Kale, Adam Roberts, and Colin Raffel. ByT5: Towards a token-free future with pre-trained byte-to-byte models. *arXiv:2105.13626 [cs]*, March 2022. URL <http://arxiv.org/abs/2105.13626>. arXiv: 2105.13626.

François Yergeau. Utf-8, a transformation format of iso 10646. Technical report, 2003.

Lili Yu, Daniel Simig, Colin Flaherty, Armen Aghajanyan, Luke Zettlemoyer, and Mike Lewis. MEGABYTE: Predicting Million-byte Sequences with Multiscale Transformers. In *Thirty-seventh Conference on Neural Information Processing Systems*, 2023. URL <https://openreview.net/forum?id=JTm02V9Xpz>.

Songming Zhang, Xue Zhang, Zengkui Sun, Yufeng Chen, and Jinan Xu. Dual-Space Knowledge Distillation for Large Language Models. In Yaser Al-Onaizan, Mohit Bansal, and Yun-Nung Chen (eds.), *Proceedings of the 2024 Conference on Empirical Methods in Natural Language Processing*, pp. 18164–18181, Miami, Florida, USA, November 2024. Association for Computational Linguistics. doi: 10.18653/v1/2024.emnlp-main.1010. URL <https://aclanthology.org/2024.emnlp-main.1010/>.

Wanjun Zhong, Ruixiang Cui, Yiduo Guo, Yaobo Liang, Shuai Lu, Yanlin Wang, Amin Saied, Weizhu Chen, and Nan Duan. Agieval: A human-centric benchmark for evaluating foundation models, 2023.

Jeffrey Zhou, Tianjian Lu, Swaroop Mishra, Siddhartha Brahma, Sujoy Basu, Yi Luan, Denny Zhou, and Le Hou. Instruction-following evaluation for large language models. *arXiv preprint arXiv:2311.07911*, 2023.

A Proofs

A.1 Incrementality Implies Unbiasedness

Let $t \in \mathcal{V}^*$ be an arbitrary token sequence and $B_T(D(t))_n = 1$, i.e. B_T is incremental at the position of the last byte in $D(t)$. Let us assume t is biased. Then $\mathcal{X}(x) \neq \emptyset$. Let $\hat{x} \in \mathcal{X}(x)$. Then $B_T(\hat{x})_n = B_T(x)_n = 1$ since x is a prefix of \hat{x} (by property (ii) of cover encodings) and B_T is incremental at the index $n = |x| - 1$. We can thus write $T(\hat{x}) = u \odot v$ for $u, v \in \mathcal{V}^+$ where u are all tokens up to and including the byte at position n . This implies that $x = D(u)$ and consequently x is a prefix of $D(u \odot v)$ for all $v \in \mathcal{V}^*$. This violates property (iii) of cover encodings (x is not a prefix of $D(u_{0:|u|-1})$) so $\hat{x} \notin \mathcal{X}(x)$, which contradicts our initial assumption. \square

A.2 Relation of the Binarized f -divergence to the Categorical f -divergence

Recall that we define the divergence induced by f as $D_f(p||q) = \sum_{x \sim D} f(p(x)||q(x))$. Here, f must be writable as $f(p(x)||q(x)) = q(x)g\left(\frac{p(x)}{q(x)}\right)$ where g is convex and non-negative by the definition of f -divergence (Rényi, 1961). The binarised f -divergence is $D_f^{\text{binarised}}(p||q) = f(p(x)||q(x)) + f(1 - p(x)||1 - q(x))$ for some $x \sim D$. We will show that the binarised f -divergence is a lower bound to the categorical f -divergence. We have

$$\begin{aligned} D_f(p||q) &= \sum_{x \sim D} f(p(x)||q(x)) \\ &= f(p(x)||q(x)) + \sum_{x' \sim D \setminus \{x\}} f(p(x')||q(x')) \quad \text{splitting the divergence into two parts} \end{aligned}$$

Since the first term of the split D_f and $D_f^{\text{binarised}}$ is the same, it remains to show that

$$f(1 - p(x)||1 - q(x)) \leq \sum_{x' \sim D \setminus \{x\}} f(p(x')||q(x'))$$

We expand $1 - p(x)$ and $1 - q(x)$ and insert $q(x)g\left(\frac{p(x)}{q(x)}\right) = f(p(x)||q(x))$

Table 5: Sensitivity of different methods to the learning rate on transfer of Gemma 2 2B IT to the Qwen2 Tokenizer by training for 5k steps (and otherwise matching the experiments in Use Case 1).

Method	Learning Rate	Benchmark								Avg.
		PiQA	ARC-C	BoolQ	MMLU	Arith.	AGI-EN	AGI-ZH	IFEval	
SFT	$2e-6$	76.1	40.4	81.6	50.3	63.9	33.6	29.6	48.3	53.0
	$1e-5$	76.7	41.1	80.5	49.6	67.2	33.5	29.4	50.5	53.6
	$5e-5$	76.4	41.3	77.5	49.7	32.4	31.4	29.2	54.2	49.0
DSKD	$2e-6$	75.0	38.1	72.0	49.0	82.3	32.0	30.2	39.0	52.2
	$1e-5$	74.6	38.7	81.0	48.1	54.8	33.0	30.7	49.0	51.2
	$5e-5$	75.3	40.4	79.3	49.6	65.5	31.5	28.5	56.5	53.3
MinED	$2e-6$	75.9	40.6	81.3	50.3	54.9	33.5	29.6	48.9	51.9
	$1e-5$	76.2	41.3	80.6	49.8	66.1	33.4	29.2	53.7	53.8
	$5e-5$	76.4	42.6	78.1	50.1	49.5	31.4	29.4	56.2	51.7
ALM	$2e-6$	75.1	43.3	82.8	50.9	85.3	36.7	30.8	56.6	57.7
	$1e-5$	76.0	44.3	82.9	52.9	86.5	37.9	32.4	55.8	58.6
	$5e-5$	76.3	43.8	82.0	52.7	80.6	37.1	31.6	54.5	57.3

$$g \left(\frac{\sum_{x' \sim D \setminus \{x\}} p(x')}{\sum_{x' \sim D \setminus \{x\}} q(x')} \right) \cdot \sum_{x' \sim D \setminus \{x\}} q(x') \leq \sum_{x' \sim D \setminus \{x\}} g \left(\frac{p(x')}{q(x')} \right) q(x')$$

which is true by Jensen’s inequality since g is convex. \square

Alternatively, it follows from the data processing inequality that the binarised f -divergence is a lower bound to the categorical f -divergence since post-processing (by merging all but two options) can only decrease the divergence. Since $D_f^{\text{binarised}}(p||q)$ is an f -divergence, the important properties that $D_f^{\text{binarised}}(p||q) = 0$ iff $p = q$ and $D_f^{\text{binarised}}(p||q) > 0$ otherwise also hold.

B Ablations & Sensitivity Analyses

B.1 Sensitivity to the Learning Rate and Distillation Coefficient β

We analyse the impact of different choices for the learning rate across different methods in Table 5 in shorter runs training for 5k steps instead of the 20k steps we train for in our main experiments. The methods are generally robust to different choices for the learning rate, although we occasionally observed loss spikes when choosing too high a learning rate in preliminary experiments. Accordingly, we set the learning rate to $1e-5$ for all methods in our main experiments since it performs consistently well. Surprisingly, some of the shorter runs from Table 5 perform better on average than the longer main runs for the non-ALM methods; this seems to be due to instances of catastrophic forgetting when training too long (which do not occur with our method). For consistency, we still report the full runs with 20k training steps as our main results. Furthermore, another important hyperparameter for the methods combining next-token prediction with a distillation loss (DSKD, MinED, and ALM + SFT) is the coefficient β used to modulate the contribution of the distillation objective via $\mathcal{L}^{\text{total}} = \mathcal{L}^{\text{SFT}} + \beta \cdot \mathcal{L}^{\text{distil}}$. We analyse the impact of different choices for β on DSKD and MinED in Table 6. MinED is robust to different choices of β , while DSKD collapses with $\beta = 3$. We choose $\beta = 1$ for our main experiments.

B.2 Impact of the Choice for the Distance Function f and the Temperature τ

The distance function f and the temperature τ are two crucial hyperparameters of our method. We analyse two choices of f , the KL-Divergence $f_{\text{KL}}(p^{1/\tau}||q^{1/\tau}) = p^{1/\tau} \log \frac{p^{1/\tau}}{q^{1/\tau}}$ and the total variation distance $f_{\text{TVD}}(p^{1/\tau}||q^{1/\tau}) = |p^{1/\tau} - q^{1/\tau}|$ across a range of temperatures. Figures 3 and 4 show the gradients w.r.t. $\log q$ over the binarised outcomes of f_{KL} and f_{TVD} , respectively. For small temperatures (e.g., $\tau = 1$), the gradient vanishes as $\log p$ or $\log q$ decreases. In general, this expected behaviour: mismatches in higher p or q should generally result in a higher contribution to the loss gradients than mismatches when p and q are both low. However, importantly, our method operates on

Table 6: Sensitivity to the distillation coefficient β on transfer of Gemma 2 2B IT to the Qwen2 Tokenizer by training for 5k steps (and otherwise matching the experiments in Use Case 1).

Method	Distillation Coefficient β	Benchmark								Avg.
		PiQA	ARC-C	BoolQ	MMLU	Arith.	AGI-EN	AGI-ZH	IFEval	
SFT		76.7	41.1	80.5	49.6	67.2	33.5	29.4	50.5	53.6
DSKD	$\beta = 1/3$	75.6	40.3	80.2	49.1	65.7	33.5	30.6	53.7	53.6
	$\beta = 1$	74.6	38.7	81.0	48.1	54.8	33.0	30.7	49.0	51.2
	$\beta = 3$	49.5	22.7	37.8	22.9	0.0	23.9	26.9	0.0	23.0
MinED	$\beta = 1/3$	76.3	40.9	80.5	49.6	66.5	33.7	29.3	51.7	53.6
	$\beta = 1$	76.2	41.3	80.6	49.8	66.1	33.4	29.2	53.7	53.8
	$\beta = 3$	76.3	41.0	80.6	50.1	65.8	34.1	29.2	54.3	53.9

Table 7: Sensitivity to the distance function f and temperature τ on transfer of Gemma 2 2B IT to the Qwen2 Tokenizer by training for 5k steps (and otherwise matching the experiments in Use Case 1).

Distance function f	Temperature τ	Benchmark								Avg.
		PiQA	ARC-C	BoolQ	MMLU	Arith.	AGI-EN	AGI-ZH	IFEval	
$f = f_{\text{KL}}$	$\tau = 1$	73.8	41.6	81.8	50.7	84.2	36.6	29.6	54.4	56.6
	$\tau = 5$	75.1	42.1	83.0	51.8	85.9	37.7	31.9	53.9	57.7
	$\tau = 100$	76.0	44.3	82.9	52.9	86.5	37.9	32.4	55.8	58.6
	$\tau \rightarrow \infty$	75.7	43.9	82.5	52.6	85.8	34.7	31.2	56.9	57.9
$f = f_{\text{TVD}}$	$\tau = 1$	73.2	43.7	83.2	52.2	84.0	38.1	33.3	53.0	57.6
	$\tau = 5$	75.7	45.0	83.1	53.5	82.8	39.5	31.3	57.2	58.5
	$\tau = 100$	76.7	46.2	82.9	53.6	84.0	38.9	32.2	60.3	59.3
	$\tau \rightarrow \infty$	77.0	46.0	82.9	53.5	83.9	38.4	32.5	60.0	59.3

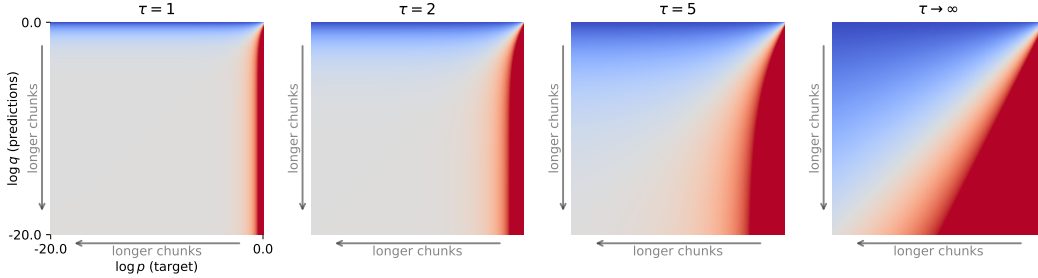


Figure 3: The KL-Divergence gradients $\frac{\delta f_{\text{KL}}(p^{1/\tau}) \|q^{1/\tau}\| + \delta f_{\text{KL}}(1-p^{1/\tau}) \|1-q^{1/\tau}\|}{\delta \log q}$ over τ .

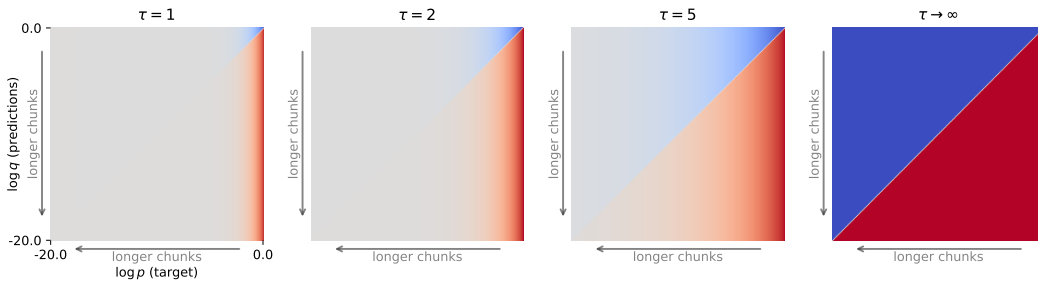


Figure 4: The Total Variation Distance gradients $\frac{\delta f_{\text{TVD}}(p^{1/\tau}) \|q^{1/\tau}\| + \delta f_{\text{TVD}}(1-p^{1/\tau}) \|1-q^{1/\tau}\|}{\delta \log q}$ over τ .

chunks of tokens and the likelihood of a chunk multiplicatively decreases as the length of the chunk increases (since the likelihood of any token is always less than 1); this means that the contribution of longer chunks to the loss vanishes if the temperature τ is low. The value of τ thus defines a trade-off: low τ leads to focusing on high-likelihood chunks. Increasing τ leads to increased focus

on lower-likelihood/longer chunks.¹⁶ We also observe notable behaviour of the KL-Divergence and Total Variation Distance as $\tau \rightarrow \infty$, and that the gradients as $\tau \rightarrow \infty$ can be computed in closed form. Specifically, $f_{\text{KL}}(p^{1/\tau} \| q^{1/\tau}) + f_{\text{KL}}(1 - p^{1/\tau} \| 1 - q^{1/\tau}) \approx C((\log p - \log q) + \log(p) \log(\frac{\log q}{\log p}))$ and $f_{\text{TVD}}(p^{1/\tau} \| q^{1/\tau}) + f_{\text{TVD}}(1 - p^{1/\tau} \| 1 - q^{1/\tau}) \approx C|\log p - \log q|$ as $\tau \rightarrow \infty$. To show this, we will use the fact that $\exp(x) \approx 1 + x$ for small enough x and let $a = \log p^{1/\tau} = \log(p)/\tau$ and $b = \log q^{1/\tau} = \log(q)/\tau$, both of which are close to zero since $\tau \rightarrow \infty$. We have

$$\begin{aligned}
f_{\text{KL}}(p^{1/\tau} \| q^{1/\tau}) &= p^{1/\tau} \log \frac{p^{1/\tau}}{q^{1/\tau}} \\
&= \exp(a)(\log \exp(a) - \log \exp(b)) \\
&= \exp(a)(a - b) \\
&\approx (1 + a)(a - b) \quad \text{since } \tau \rightarrow \infty \\
&= a + a^2 - b - ab \\
&= \log(p)/\tau + \log(p)^2/\tau^2 - \log(q)/\tau - \log(p) \log(q)/\tau^2 \\
&\approx (\log(p) - \log(q))/\tau \quad \text{since } 1/\tau \gg 1/\tau^2 \\
&= C(\log p - \log q) \quad \text{where the constant } C = 1/\tau
\end{aligned}$$

and

$$\begin{aligned}
f_{\text{KL}}(1 - p^{1/\tau} \| 1 - q^{1/\tau}) &= (1 - p^{1/\tau}) \log \frac{(1 - p^{1/\tau})}{(1 - q^{1/\tau})} \\
&= (1 - \exp(a))(\log(1 - \exp(a)) - \log(1 - \exp(b))) \\
&\approx -a(\log(-a) - \log(-b)) \quad \text{since } \tau \rightarrow \infty \\
&= \log(p)(\log(-\log q) - \log(-\log p))/\tau \\
&= C \left(\log(p) \log \left(\frac{\log q}{\log p} \right) \right) \quad \text{where the constant } C = 1/\tau
\end{aligned}$$

Analogously, for the Total Variation Distance we have

$$\begin{aligned}
f_{\text{TVD}}(p^{1/\tau} \| q^{1/\tau}) &= f_{\text{TVD}}(1 - p^{1/\tau} \| 1 - q^{1/\tau}) = |p^{1/\tau} - q^{1/\tau}| \\
&= |\exp(a) - \exp(b)| \\
&\approx |(1 + a) - (1 + b)| \quad \text{since } \tau \rightarrow \infty \\
&= |a - b| \\
&= |\log(p)/\tau - \log(q)/\tau| \\
&= C|\log(p) - \log(q)| \quad \text{where the constant } C = 1/\tau
\end{aligned}$$

Empirically, both KL-divergence and Total Variation Distance perform well, and higher τ is beneficial (Table 7). Although Total Variation Distance scores slightly higher than the KL-divergence in the best case in these experiments, we opt for the KL-divergence for our main experiments to preserve the desirable property of higher contribution to the loss by higher-probability chunks.

B.3 Impact of Outcome Chunk Debiasing & Impact of the Embedding Projector

We ablate the empirical impact of Outcome Chunk Debiasing in Table 8, finding strong improvements on the generative IFEval task and otherwise comparable results. Figure 5 shows an example where Outcome Chunk Debiasing leads to a large difference in the compared likelihoods. In the same Table 8, we ablate the impact of the Embedding Projector, also finding especially substantial improvements

¹⁶Disentangling the loss contribution by longer chunks compared to shorter lower-likelihood chunks could be an avenue for future work.

Table 8: Effect of removing Outcome Chunk Debiasing and of removing the Embedding Projector on transfer of Gemma 2 2B IT to the Qwen2 Tokenizer.

Method	Benchmark								
	PiQA	ARC-C	BoolQ	MMLU	Arith.	AGI-EN	AGI-ZH	IFEval	Avg.
ALM	76.9	46.9	82.8	53.8	83.9	38.8	32.3	62.5	59.8
ALM w/o Outcome Chunk Debiasing	75.8	45.7	82.6	53.4	84.9	39.1	32.8	55.9	58.8
ALM w/o Embedding Projector	77.3	46.8	83.1	53.6	84.2	38.2	32.7	59.0	59.4

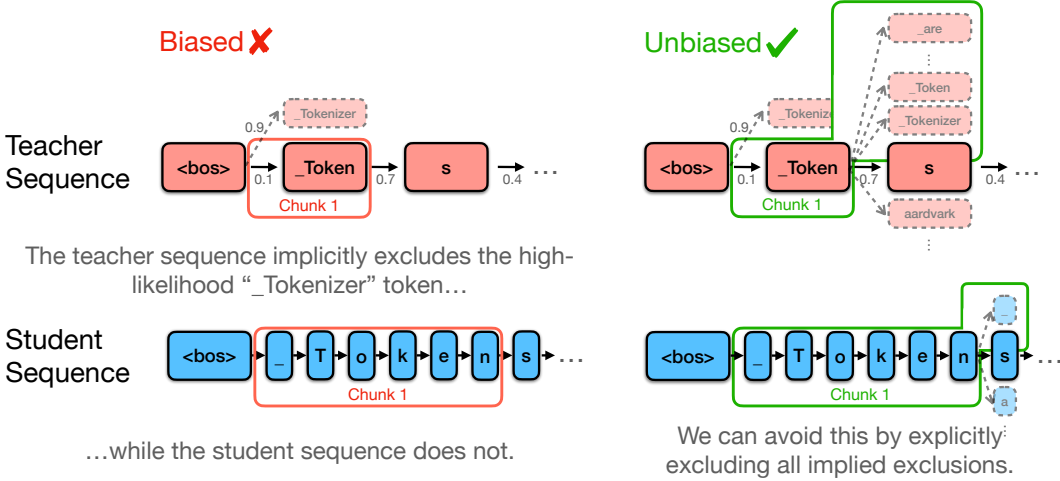


Figure 5: Outcome Chunk Debiasing avoids biases stemming from the outcome chunks having different implied exclusions.

on IFEval; however, throughout testing leading up to our final results, we have observed consistent improvements across different settings from including the Embedding Projector.

Embedding Projector Architecture. For the embedding projector, we follow the architecture of the hypernetwork introduced by Minixhofer et al. (2024) (which can be seen as an embedding projector with varying inputs) using 3 layers, 12 attention heads and an intermediate size equal to 2x the hidden dimension. The cost of the projection is negligible compared to the time it takes to run the main model, and the embedding projector can be discarded after training. One modification we make is that we initialize the last layer’s weight matrix in the projector to zeros and residually add the last layer’s predictions to the original embedding matrix to make sure the projector’s predictions are equal to the original embeddings at the start of training (otherwise, a separate warmup phase as in Minixhofer et al. (2024) would be necessary).

B.4 Sensitivity to the bias threshold γ

We quantify the sensitivity to the bias threshold γ in Table 9. Notably, very long chunks (e.g., via $\gamma = 0$) still enable successful training, albeit moderately degrading performance.

Table 9: Effect of varying the bias threshold γ on transfer of Gemma 2 2B IT to the Qwen2 Tokenizer. Avg. *Chunk Length* denotes the average length in tokens of the student and the teacher chunks.

Threshold γ	Avg. Chunk Length		Benchmark								
	Teacher	Student	PiQA	ARC-C	BoolQ	MMLU	Arith.	AGI-EN	AGI-ZH	IFEval	Avg.
$\gamma = 1$	1.1	1.1	76.2	45.9	82.4	53.5	81.1	39.0	31.1	56.2	58.2
$\gamma = 1e-3$	2.4	2.4	76.9	44.4	80.9	53.0	84.0	38.5	33.8	56.4	58.5
$\gamma = 1e-4$	5.7	5.7	76.9	46.9	82.8	53.8	83.9	38.8	32.3	62.5	59.8
$\gamma = 1e-5$	12.3	12.3	76.4	44.2	82.0	53.4	82.7	37.3	31.1	57.4	58.1
$\gamma = 0$	178.6	179.6	75.2	45.6	82.8	53.4	85.3	37.0	31.4	58.4	58.6